Spectrochimica Acta Part A 86 (2012) 231–241

Contents lists available at SciVerse ScienceDirect

Spectrochimica Acta Part A: Molecular and Biomolecular Spectroscopy

journal homepage: www.elsevier.com/locate/saa

Structural, vibrational and hyperpolarizability calculation of (*E*)-2-(2-hydroxybenzylideneamino)-3-methylbutanoic acid

S. Subashchandrabose[a], H. Saleem[a,*], Y. Erdogdu[b], Ö. Dereli[c], V. Thanikachalam[d], J. Jayabharathi[d]

[a] Department of Physics, Annamalai University, Annamalai Nagar, Tamil Nadu 608002, India
[b] Department of Physics, Ahi Evran University, 40040 Kirsehir, Turkey
[c] A. Keleşoğlu Education Faculty, Department of Physics, Selcuk University, 42090 Konya, Turkey
[d] Department of Chemistry, Annamalai University, Annamalai Nagar, Tamil Nadu 608002, India

ARTICLE INFO

Article history:
Received 26 August 2011
Received in revised form
28 September 2011
Accepted 14 October 2011

Keywords:
FT-Raman
FT-IR
TED
NBO
Leucine

ABSTRACT

The (*E*)-2-(2-hydroxybenzylideneamino)-3-methylbutanoic acid (*E*)-2HBAMBA was synthesized. The FT-IR, FT-Raman and UV–vis spectra have been recorded and characterized. Theoretical wavenumbers along with IR and Raman intensities were calculated using B3LYP/6-31G(d,p) level and total energy distribution (TED) of the various normal mode of vibrations were also studied. The conformational analysis was performed for a stable conformer by selecting the dihedral angles and the optimized bond parameters were calculated for the stable structure. Effect of intramolecular interactions is calculated by changing the orientation of hydroxyl hydrogen. To know the charge transfer while changing the hydroxyl group hydrogen orientation, the NBO analysis was performed. Using the same level of calculation, the electronic charge transfers were calculated and compared.

1. Introduction

Schiff-base compounds exhibit a wide range of biological activities [1–3], anti-HIV [4–6], anti-tumor activities [7], and synthesis of transition metal complexes [8–11]. Very often it undergoes a variety of chemical reactions, being as a key precursor for new compounds exhibiting diverse molecular structures and properties [12–14]. It is worth mentioning that the salicylaldehyde moiety appears in many compounds exhibiting various biological activity, including reactants used in the design of compounds exhibiting antiviral activity [15], as well as in reactions resulting in new compounds with anticancer [16,17] or antimicrobial activity [18]. It is also present during the synthesis of new products called "aspirin-like molecules" exhibiting anti-inflammatory activity [19]. Some Schiff bases which are derived from salicylaldehyde have attracted the interest of chemists and physicists because they show thermochromism and photochromism in the solid state by proton atom transfer from the hydroxyl oxygen atom to the nitrogen atom [20]. It has been proposed that molecules showing thermochromism are planar, while those showing photochromism are non-planar [21]. In addition to its presence in many chemical reactions, salicylaldehyde has also found applications in molecular engineering [22]. Salicylaldehyde is also an interesting subject for various physico-chemical investigations; because it has four isomers, and due to internal reorganization, it can have more than one different hydrogen-bonded conformer [23]. Chandran et al. [24] recorded FT-IR and FT-Raman spectra of N-carbamimidoyl-4-((2-hydroxybenzylidene) amino) benzene sulfon-amide. In this study we are interested to find the conformational, vibrational, physical and chemical properties of (*E*)-2-(2-hydroxybenzylideneamino)-3-methylbutanoic acid.

2. Experimental

2.1. Synthesis

This compound was synthesized by mixing the salicylaldehyde in ethanol and sodium salt of L-leucine in ethanol–water (50%, v/v) [25]. The mixture was heated and refluxed on a mantel about 5 h. The reaction mixture was cooled to room temperature and neutralized by 1:1 HCL. The white Schiff base was separated, filtered off, washed thoroughly with deionised water ethanol mixture followed by ether wash. The product obtained was dried over vacuum desiccators. The melting point of the compound is 114 °C (lit. 114 °C)

* Corresponding author. Tel.: +91 9443879295.
E-mail addresses: sscbphysics@gmail.com, saleem_h2001@yahoo.com (H. Saleem).

1386-1425/$ – see front matter © 2011 Elsevier B.V. All rights reserved.
doi:10.1016/j.saa.2011.10.029

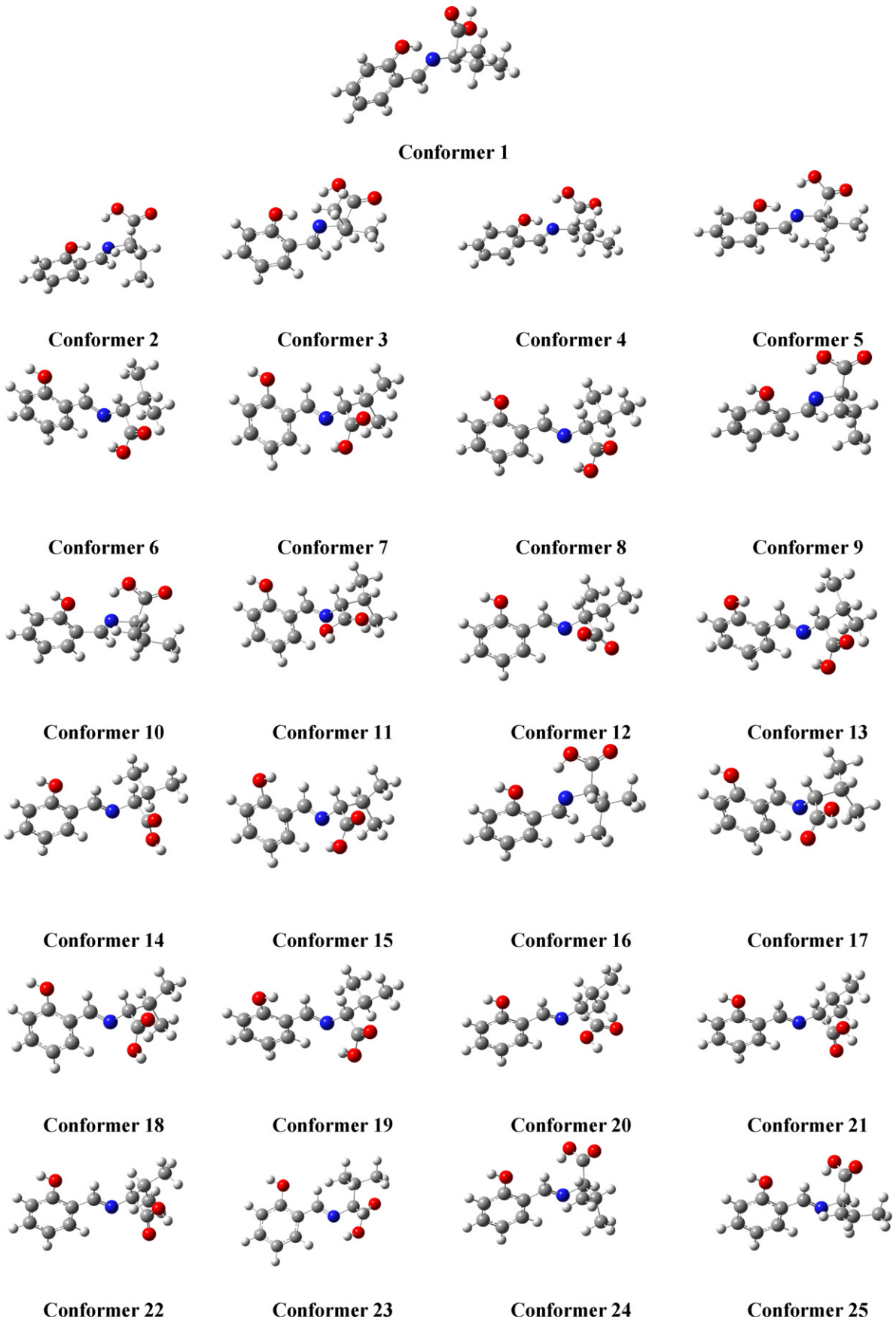

Fig. 1. All possible conformers of (*E*)-2-(2-hydroxybenzylideneamino)-3-methylbutanoic acid.

Table 1
Energetics of the conformers calculated at the B3LYP/6-31G(d,p) level.

Conf.	E (Hartree)	ΔE (kcal/mol)	E_0 (Hartree)	ΔE_0 (kcal/mol)	Dip. mom. (D)
1	−746.77616261	0.0000000	−746.5207820	0.000000	3.4607
2	−746.77612700	0.0223456	−746.5206390	0.089734	5.1685
3	−746.77506194	0.6906809	−746.5193890	0.874121	4.9098
4	−746.77505988	0.6919736	−746.5194340	0.845883	4.9973
5	−746.77454976	1.0120787	−746.5190200	1.105672	4.7913
6	−746.76502804	6.9870485	−746.5099310	6.809106	7.5704
7	−746.76460803	7.2506087	−746.5094370	7.119095	7.5454
8	−746.76380339	7.7555280	−746.5087600	7.543919	7.2458
9	−746.76191548	8.9402094	−746.5069290	8.692889	7.0849
10	−746.76161203	9.1306272	−746.5065900	8.905615	7.0769
11	−746.76149997	9.2009459	−746.5068440	8.746227	4.1968
12	−746.76149076	9.2067253	−746.5068080	8.768818	4.1967
13	−746.76122573	9.3730341	−746.5064770	8.976523	4.8911
14	−746.76107620	9.4668656	−746.5064980	8.963346	2.932
15	−746.76076240	9.6637781	−746.5059360	9.316006	4.8197
16	−746.76068747	9.7107974	−746.5056780	9.477903	6.8361
17	−746.76062022	9.7529974	−746.5061370	9.189877	2.8792
18	−746.76025759	9.9805511	−746.5054750	9.605288	3.536
19	−746.76005683	10.1065300	−746.5054000	9.652351	4.6735
20	−746.76004226	10.1156728	−746.5053690	9.671804	4.2924
21	−746.75959110	10.3987800	−746.5049060	9.962341	3.5117
22	−746.75959070	10.3990310	−746.5048980	9.967361	3.5372
23	−746.75387108	13.9881468	−746.4987290	13.83847	6.3718
24	−746.75156353	15.4361564	−746.4967840	15.05897	5.2887
25	−746.75049738	16.1051756	−746.4956800	15.75174	5.0138

E_0, zero point corrected energy.

[25]. Microanal. CalCd % for C13H17NO3; C, 66.38; H, 7.23; N, 5.95; found C, 66.23; H, 7.20; N, 5.85.

2.2. FT-Raman and FT-IR spectra

The FT-Raman spectrum of (*E*)-2HBAMBA was recorded using the 1064 nm line of a Nd:YAG laser as excitation wavelength in the region 10–3500 cm^{-1} on a Bruker model IFS 66V spectrophotometer equipped with an FRA 106 FT-Raman module accessory. The spectral measurements were carried out at Sree Chitra Tirunal Institute for Medical Sciences and Technology, Poojappura, Thiruvananthapuram, Kerala, India. The FT-IR spectrum of this compound was recorded in the region 400–4000 cm^{-1} on an IFS 66V spectrophotometer using the KBr pellet technique. The spectrum was recorded at room temperature, with a scanning speed of 10 cm^{-1} min^{-1} and at the spectral resolution of 2.0 cm^{-1} in CISL Laboratory, Annamalai University, Tamilnadu, India.

3. Computational details

In order to establish the stable possible conformations, the conformational space of title compound was scanned with molecular mechanic simulations. This calculation was performed with the Spartan 08 program [26]. For meeting the requirements of both accuracy and computing economy, theoretical methods and basis sets should be considered. Density functional theory (DFT) has been proved to be extremely useful in treating electronic structure of molecules. The basis set 6-31G(d,p) was used as a effective and economical level to study fairly large organic molecules. After the most stable conformer of the title compound determined, geometry optimizations of this conformer have been performed by using Gaussian 03W [27] program package, invoking gradient geometry optimization [27,28]. Initial geometry generated from standard geometrical parameters was minimized without any constraint in the potential energy surface at DFT level, adopting the standard 6-31G(d,p) basis set. The optimized structural parameters were used in the vibrational frequency calculations at the DFT levels to characterize all stationary points as minima. Then, vibrationally averaged nuclear positions of (*E*)-2HBAMBA was used for harmonic vibrational frequency calculations resulting in IR and Raman frequencies together with intensities and Raman depolarization ratios. In this study, the DFT method (B3LYP) has been used for the computation of molecular structure, vibrational frequencies and energies of optimized structures. By combining the results of the GAUSSVIEW program [29] with symmetry considerations, vibrational frequency assignments were made with a high degree of accuracy using SQM program [30].

It should be noted that Gaussian 03W package able to calculate the Raman activity. The Raman activities were transformed into Raman intensities using Raint program [31] by the expression:

$$I_i = 10^{-12} \times (\nu_0 - \nu_i)^4 \times \frac{1}{\nu_i} \times \mathrm{RA}_i \quad (1)$$

where I_i is the Raman intensity, RA_i is the Raman scattering activities, ν_i is the wavenumber of the normal modes and ν_0 denotes the wavenumber of the excitation laser [32].

4. Results and discussion

4.1. Conformational analysis

To found stable conformers, a meticulous conformational analysis was carried out for the title compound. Rotating 10 each degree intervals around the free rotation bonds, conformational space of the title compound was scanned by molecular mechanic simulations and then full geometry optimizations of these structures were performed by B3LYP/6-31G(d,p) method. Results of geometry optimizations were indicated that the title compound is rather flexible molecule and, in theory, may have at least twenty five conformers as shown in Fig. 1. Ground state energies, zero point corrected energies (Eelect. + ZPE), relative energies and dipole moments of conformers were presented in Table 1. Optimized molecular structure and atomic numbering is given in Fig. 2. Zero point corrections have not caused any significant changes in the stability order. From both the calculated energies of twenty five conformers, given in Table 1, the conformer 1 is the most stable and the comparison of the theoretical and experimental geometry of the title compound,

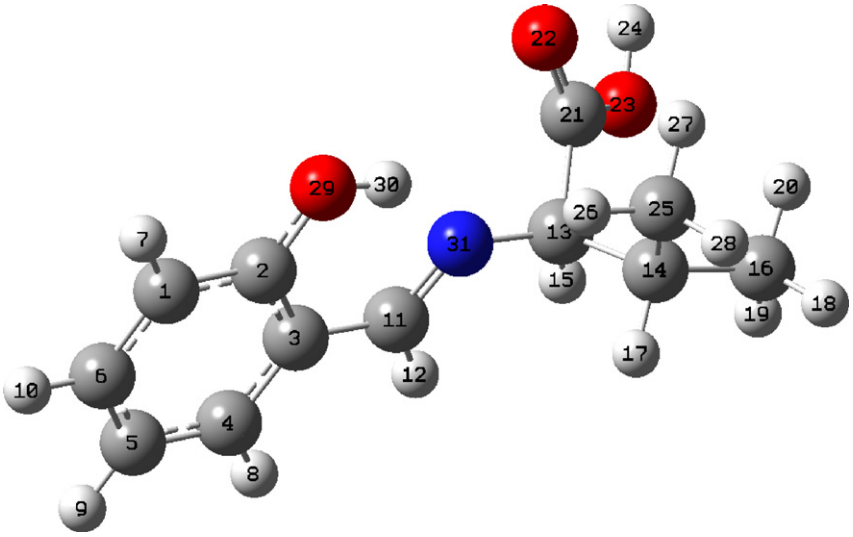

Fig. 2. The optimized molecular structure of (*E*)-2-(2-hydroxybenzylideneamino)-3-methylbutanoic acid.

Table 2
The geometric bond length, bond angle and dihedral angle of (*E*)-2HBAMBA.

Parameters	B3LYP/6-31G(d,p)	Experimental		
		a	*b*	*c*
Bond lengths (Å)				
C_1–C_2	1.405			1.386
C_1–C_6	1.388			1.366
C_1–H_7	1.085			0.930
C_2–C_3	1.424		1.411	1.402
C_2–O_{29}	1.339	1.349		1.352
C_3–C_4	1.408			1.400
C_3–C_{11}	1.453	1.410	1.433	1.467
C_4–C_5	1.386			1.357
C_4–H_8	1.088			0.910
C_5–C_6	1.404			1.372
C_6–H_{10}	1.086			0.940
C_{11}–N_{31}	1.286	1.278	1.296	
C_{13}–C_{14}	1.566			
C_{13}–C_{21}	1.528			
C_{13}–N_{31}	1.450		1.450	
C_{14}–C_{16}	1.535			
C_{14}–C_{25}	1.534			
C_{21}–O_{22}	1.209			
C_{21}–O_{23}	1.357	1.358	1.352	
O_{23}–H_{24}	0.973			
O_{29}–H_{30}	0.998			
($H_{30}\cdots N_{31}$)	1.722		1.873	
Bond angles (°)				
C_2–C_1–C_6	120.2			121.0
C_1–C_2–C_3	119.1			119.2
C_1–C_2–O_{29}	118.6			123.4
C_3–C_2–O_{29}	122.2			119.0
C_2–C_3–C_4	119.1			119.3
C_2–C_3–C_{11}	120.7			120.0
C_4–C_3–C_{11}	120.1			119.1
C_3–C_4–C_5	121.2			120.7
C_4–C_5–C_6	119.0			122.4
C_1–C_6–C_5	121.1			119.0
Dihedral angles (°)				
C_6–C_1–C_2–C_3	−0.100			
C_6–C_1–C_2–O_{29}	179.8			
H_7–C_1–C_2–C_3	179.9			
C_2–C_1–C_6–H_{10}	−179.9			

a, *b*, *c* are taken from Refs. [33–35].

given in Table 2, shows that optimized geometry of conformer 1 (namely conformer 1 appears in the solid state) fairly well reproduce the experimental one, from this point the discussion will be based on conformer 1, further in this paper.

4.2. Molecular geometric

The x-ray diffraction data of literature [33,34] had shown the C=N and C–N bond length is about 1.296, 1.278 Å and 1.433, 1.410 Å, respectively. In this present study, the C=N and C–N are calculated at about 1.286 and 1.450. The deviation of bond length between C=N and C–N is due to electron engagement in C=N. According to Tezer and Karakus [35], the intra-molecular interaction has been found in this title compound between (O29–H30···N31) nitrogen and adjacent hydroxyl hydrogen atoms and its calculated distance is about 1.722 (B3LYP). This intra-molecular bond length has shown an agreement with literature [33,35]. The carbon–carbon bond distances are not equal in this molecule, namely C1–C2 (1.405), C1–C6 (1.388), C3–C11 (1.424), C3–C4 (1.408) and C3–C11 (1.453 Å). Reasoning of differences is the conjugative effect is exists in this molecule. The transfer of hydrogen atom from nitrogen to oxygen atom is accompanied by a rearrangement of the whole six-membered ring, and substantial changes are observed in the C–O and C–N bonds [35]. The bond length of keto (C=O) group is calculated about 1.209 (B3LYP) whereas the C–O is calculated about 1.357 (B3LYP). The C=O bond length is smaller than the single bond (C–O) [35]. The effect of intra-molecular interaction the O29–H30 bond length is appreciably deviates from O23–H24 bond. From this observation the O29–H30 bond distance is increased by 0.025 Å from the O23–H24. This is also the further evidence for the intra-molecular hydrogen bonding interaction in the present molecule.

4.3. Vibrational assignments

In order to obtain the spectroscopic results for (*E*)-2HBAMBA we have performed vibrational frequency calculation on the stable conformer. The present molecule has 31 atoms; hence one can have 87 normal modes of vibrations. All the vibrations are both IR and Raman active. To investigate the vibrations corresponding to the functional groups, the FT-IR and FT-Raman spectra are recorded, and these recorded frequencies are compared with calculated wave numbers using B3LYP/6-31G(d,p) level as basis set. Assignments are made on the basis of TED with the help of scaled quantum calculations using the same basis set. The harmonic wave numbers, IR, Raman intensities and force constants are listed in Table 3. The observed FT-IR, FT-Raman and their corresponding theoretical spectra are shown in Figs. 3 and 4, respectively.

Table 3
Vibrational wave numbers obtained for (*E*)-2HBAMBA at B3LYP/6-31G(d,p).

Mode nos.	Theoretical			Experimental		
	B3LYP[a]	I_{IR} [b]	I_{Raman} [c]	FT-IR	FT-Raman	TED%[d]
ν_1	3655	19.57	1.90	3803w		$\nu_{O29-H30}(100)$
ν_2	3594	21.87	3.40	3690w		$\nu_{O23-H24}(100)$
ν_3	3087	9.88	6.62	3095w		$\nu_{C5-H9}(73)+\nu_{C6-H10}(21)$
ν_4	3069	6.67	2.84			$\nu_{C5-H9}(18)+\nu_{C6-H10}(72)$
ν_5	3053	2.31	1.69			$\nu_{C4-H8}(90)$
ν_6	3039	7.12	2.14			$\nu_{C1-H7}(93)$
ν_7	3026	5.65	1.14			$\nu_{C25-H26}(81)+\nu_{C25-H27}(15)$
ν_8	2998	24.64	3.11			$\nu_{C16-H18}(11)+\nu_{C16-H20}(11)+\nu_{C25-H27}(42)+\nu_{C25-H28}(32)$
ν_9	2992	5.38	1.25		2994m	$\nu_{C16-H18}(57)+\nu_{C16-H19}(13)+\nu_{C16-H20}(12)+\nu_{C25-H27}(10)$
ν_{10}	2991	12.33	1.25	2954w		$\nu_{C16-H19}(50)+\nu_{C16-H20}(43)$
ν_{11}	2931	16.37	5.61	2932w	2932s	$\nu_{C25-H26}(16)+\nu_{C25-H27}(28)+\nu_{C25-H28}(51)$
ν_{12}	2923	13.17	2.21			$\nu_{C16-H18}(29)+\nu_{C16-H19}(34)+\nu_{C16-H20}(32)$
ν_{13}	2908	8.87	2.34		2896w	$\nu_{C14-H17}(97)$
ν_{14}	2857	27.35	1.99	2868w	2868vs	$\nu_{C13-H15}(98)$
ν_{15}	2845	20.65	1.02			$\nu_{C11-H12}(98)$
ν_{16}	1776	100.00	0.61	1616s		$\nu_{C21=O22}(86)$
ν_{17}	1662	86.27	70.83	1586w	1586s	$\nu_{C11-N31}(78)$
ν_{18}	1597	25.13	26.62			$\nu_{C2-C1}(18)+\nu_{C4-C3}(13)+\nu_{C5-C4}(22)+\nu_{C6-C1}(13)$
ν_{19}	1574	19.20	20.13		1563m	$\nu_{C3-C2}(21)+\nu_{C6-C1}(13)+\nu_{C6-C5}(21)$
ν_{20}	1488	7.47	6.63	1513s	1516w	$\nu_{C6-C5}(10)+\delta_{C2-C1-H7}(10)$
ν_{21}	1467	4.15	0.23	1470m	1470m	$\delta_{H26-C25-H27}(27)$
ν_{22}	1457	1.23	4.27	1455w	1453s	$\delta_{H18-C16-H19}(15)+\delta_{H18-C16-H20}(24)$
ν_{23}	1445	0.11	2.96			$\delta_{H18-C16-H19}(10)+\delta_{H26-C25-H28}(15)+\delta_{H27-C25-H28}(17)$
ν_{24}	1444	0.84	1.64			$\delta_{H19-C16-H20}(20)+\delta_{H27-C25-H28}(12)$
ν_{25}	1436	14.68	1.43	1415s	1414m	$\delta_{C6-C5-H9}(14)+\delta_{H10-C6-C5}(12)$
ν_{26}	1391	18.40	2.13			$\delta_{H12-C11-C3}(13)+\delta_{H12-C11-N31}(20)$
ν_{27}	1383	3.85	0.40			$\delta_{H18-C16-H20}(11)$
ν_{28}	1367	6.57	0.39	1360m		$\delta_{H-C-C}(25)+\delta_{H-C-H}(25)+\delta_{H2-C11-N13}(16)$
ν_{29}	1360	3.19	0.58			$\delta_{H12-C11-C3}(13)+\delta_{H12-C11-N31}(16)$
ν_{30}	1327	12.33	2.35	1340m	1341s	$\nu_{C2-C1}(10)+\nu_{C5-C4}(15)+\nu_{C6-C1}(15)+\delta_{H30-O29-C2}(18)$
ν_{31}	1324	4.56	0.67	1312m	1314m	$\Gamma_{H17-C14-C13-H15}(11)$
ν_{32}	1289	41.12	5.61	1295m	1295m	$\delta_{C2-C1-H7}(10)+\delta_{C6-C1-H7}(11)+\delta_{H30-O29-C2}(11)$
ν_{33}	1282	8.48	1.19			$\delta_{H-C-C}(11)+\delta_{C-C-H}(11)+\Gamma_{H-C-C-H}(24)$
ν_{34}	1273	7.51	1.64			$\nu_{O29-C2}(13)+\delta_{H24-O23-C21}(23)$
ν_{35}	1263	3.48	0.17			$\nu_{C4-C3}(12)+\nu_{O29-C2}(24)$
ν_{36}	1238	3.11	4.34	1236w	1236w	$\delta_{C14-C13-H15}(12)+\delta_{H24-O23-C21}(17)+\Gamma_{C-N-C-H}(12)$
ν_{37}	1203	7.85	28.85			$\nu_{C4-C3}(17)+\nu_{C11-C3}(31)+\delta_{C5-C4-H8}(10)$
ν_{38}	1161	5.38	0.46	1181w	1181w	$\delta_{H19-C16-C14}(13)+\delta_{H26-C25-C14}(12)$
ν_{39}	1153	12.05	1.24	1173w		$\nu_{C2-C1}(12)+\delta_{H30-O29-C2}(27)$
ν_{40}	1143	2.59	2.40	1140w		$\delta_{H9-C5-C4}(14)+\delta_{C6-C5-H9}(12)+\delta_{H-C-C}(35)$
ν_{41}	1126	30.57	0.26	1131vs	1130vw	$\nu_{O23-C21}(10)+\delta_{CCH}(11)$
ν_{42}	1106	97.78	0.21			$\nu_{O23-C21}(32)+\delta_{H24-O23-C21}(11)$
ν_{43}	1089	26.75	0.12	1085w	1089w	$\nu_{C5-C4}(14)+\delta_{H30-O29-C2}(13)$
ν_{44}	1072	25.33	2.29			$\delta_{H28-C25-C14}(12)$
ν_{45}	1039	15.29	1.48	1036w		$\nu_{C6-C1}(12)+\nu_{C6-C5}(26)+\delta_{N31-C13}(20)$
ν_{46}	1025	20.47	13.08	998w		$\nu_{C6-C5}(14)+\delta_{N31-C13}(37)$
ν_{47}	982	0.68	2.61		964m	$\Gamma_{H12-C11-C3-C2}(13)+\Gamma_{H12-C11-C3-C4}(20)+\Gamma_{C-N-C-H}(38)$
ν_{48}	938	0.01	0.12	942w	946m	$\Gamma_{H9-C5-C4-H8}(19)+\Gamma_{H10-C6-C1-H7}(15)+\Gamma_{H10-C6-C5-H9}(30)$
ν_{49}	935	0.29	1.69			$\nu_{C16-C14}(21)+\delta_{H18-C16-C14}(13)+\delta_{H28-C25-C14}(17)$
ν_{50}	924	0.65	2.73	925m	925m	$\nu_{C14-C13}(23)+\delta_{H19-C16-C14}(15)$
ν_{51}	910	0.88	0.48			$\delta_{H19-C16-C14}(11)+\delta_{H20-C16-C14}(16)+\delta_{H-C-C}(33)$
ν_{52}	905	0.55	0.41			$\Gamma_{H9-C5-C4-H8}(19)+\Gamma_{H10-C6-C1-H7}(14)+\Gamma_{H8-C4-C3-C11}(10)$
ν_{53}	889	4.74	1.65			$\nu_{C21-C13}(19)$
ν_{54}	848	5.04	4.54	848vs	842s	$\nu_{C21-C13}(17)$
ν_{55}	818	0.62	2.32	833s		$\Gamma_{C5-C6-C1-H7}(12)+\Gamma_{O29-C2-C1-H7}(17)$
ν_{56}	808	0.74	6.18			$\nu_{C16-C14}(12)+\nu_{C25-C14}(28)$
ν_{57}	756	5.27	3.50	774s	782w	$\nu_{C3-C2}(21)+\nu_{O29-C2}(10)$
ν_{58}	735	28.19	0.96	746w		$\Gamma_{H9-C5-C4-C3}(16)+\Gamma_{C1-C6-C5-H9}(15)+\Gamma_{H10-C6-C1-C2}(14)+\Gamma_{O29-C2-C1-H7}(12)$
ν_{59}	726	17.47	2.42	716w		$\nu_{C14-C13}(16)+\Gamma_{H24-O23-C21-O22}(20)$
ν_{60}	712	1.20	0.39			$\Gamma_{C3-C2-C1-H7}(11)$
ν_{61}	671	12.55	0.88	684vs	684w	$\nu_{O23-C21}(11)+\delta_{O22-C21-C13}(12)+\delta_{N31-C11-C3}(10)$
ν_{62}	641	9.82	3.05	670w		$\delta_{O22-C21-O23}(13)$
ν_{63}	611	34.84	2.44	611w		$\Gamma_{H24-O23-C21-C13}(38)+\Gamma_{H24-O23-C21-O22}(20)$
ν_{64}	562	6.16	1.95			$\delta_{C2-C1-C6}(11)$
ν_{65}	543	0.32	0.70	536vs	535w	$\Gamma_{C1-C6-C5-C4}(20)+\Gamma_{C6-C5-C4-C3}(12)$
ν_{66}	504	7.84	3.68			$\nu_{C-C}(13)+\delta_{C-C-C}(21)+\delta_{O-C-C}(11)$
ν_{67}	469	1.80	0.88			$\Gamma_{C-C-C-C}(27)+\Gamma_{C-C-C-H}(14)$
ν_{68}	449	2.65	1.13	454w	457m	$\delta_{O29-C2-C1}(22)+\delta_{C3-C2-O29}(14)+\delta_{C11-N31-C13}(13)$
ν_{69}	440	1.44	0.74	440s	435w	$\Gamma_{H-C-C-C}(24)$
ν_{70}	401	32.42	3.08		396w	$\Gamma_{H30-O29-C2-C1}(37)+\Gamma_{H30-O29-C2-C3}(35)$
ν_{71}	389	14.71	1.06			$\Gamma_{H30-O29-C2-C1}(10)+\Gamma_{H30-O29-C2-C3}(10)$
ν_{72}	359	2.22	0.75			$\delta_{O23-C21-C13}(14)+\delta_{C16-C14-C25}(13)+\delta_{C3-C2-O29}(11)$
ν_{73}	342	0.39	0.83		335w	$\delta_{C16-C14-C13}(10)+\delta_{C16-C14-C25}(11)+\delta_{C3-C2-O29}(11)$
ν_{74}	320	1.91	1.56			$\delta_{C25-C14-C13}(11)+\Gamma_{C13-N31-C11-C3}(10)$

Table 3 (*Continued*)

Mode nos.	Theoretical			Experimental		
	B3LYP[a]	I_{IR} [b]	I_{Raman} [c]	FT-IR	FT-Raman	TED%[d]
ν_{75}	276	8.16	2.84			$\delta_{C-C-C}(11)+\delta_{O-C-C}(12)+\delta_{C-C-N}(12)+\Gamma_{H-C-C-C}(11)$
ν_{76}	246	0.27	3.08			$\Gamma_{H26-C25-C14-C16}(10)$
ν_{77}	230	0.12	1.22			$\Gamma_{H-C-C-C}(48)$
ν_{78}	219	0.10	0.17		213w	$\Gamma_{H-C-C-C}(51)$
ν_{79}	203	0.65	0.70			$\Gamma_{C-C-C-O}(27)+\Gamma_{N31-C11-C3-C4}(10)$
ν_{80}	191	0.47	0.50		167w	$\delta_{C11-C3-C2}(14)$
ν_{81}	145	0.15	5.08		124s	$\delta_{C14-C13-C21}(39)$
ν_{82}	91	0.26	2.07			$\delta_{N31-C11-C3}(11)+\Gamma_{C-C-C-C}(24)+\Gamma_{H17-C14-C13-C21}(11)+\Gamma_{O23-C21-C13-C14}(10)$
ν_{83}	86	0.16	19.86		86vs	$\Gamma_{N31-C11-C3-C4}(16)+\Gamma_{C-N-C-C}(25)$
ν_{84}	61	0.57	9.11			$\delta_{N31-C11-C3}(11)+\delta_{C11-N31-C13}(17)+\Gamma_{C-C-C-N}(25)$
ν_{85}	44	0.91	35.46			$\Gamma_{H12-C11-C3-C2}(18)+\Gamma_{C13-N31-C11-C3}(27)+\Gamma_{C13-N31-C11-H12}(11)$
ν_{86}	28	0.67	13.42			$\Gamma_{O23-C21-C13-C14}(16)+\Gamma_{O22-C21-C13-N31}(17)+\Gamma_{O23-C21-C13-N31}(24)$
ν_{87}	23	0.08	100.01			$\Gamma_{N31-C11-C3-C2}(15)+\Gamma_{N31-C11-C3-C4}(17)+\Gamma_{C11-N31-C13-C14}(19)+\Gamma_{C11-N31-C13-C21}(18)$

ν – Stretching, δ – scissoring, Γ – torsion, s – strong, m – medium, w – weak, and v – very.

[a] Obtained from the wave numbers calculated at B3LYP/6-31G(d,p) using scaling factor 0.9608 [58].

[b] Relative absorption intensities normalized with highest peak absorption equal to 100.

[c] Relative Raman intensities normalized to 100.

[d] Total energy distribution calculated B3LYP/6-31G(d,p) level, TED less than 10% are not shown.

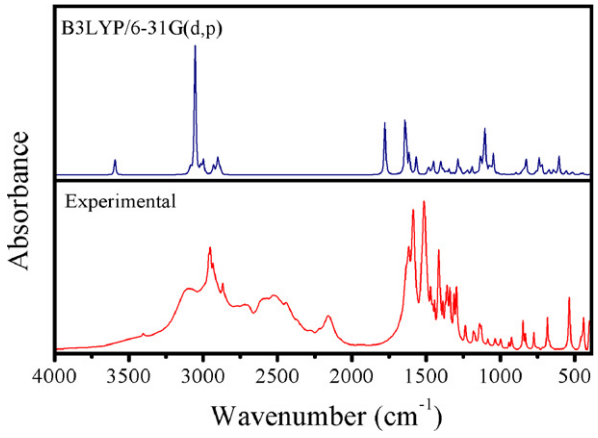

Fig. 3. The experimental and theoretical spectra of (*E*)-2HBAMBA.

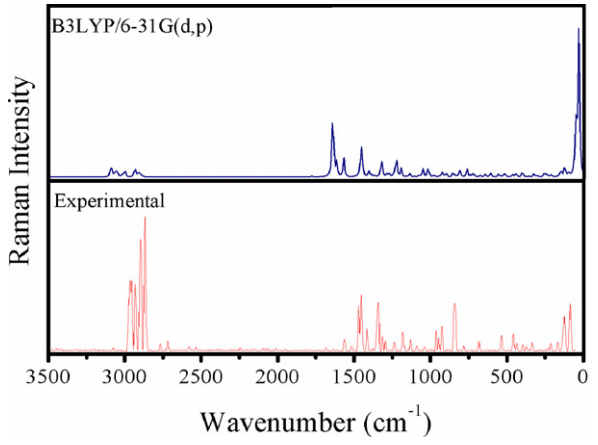

Fig. 4. The experimental and theoretical FT-Raman spectra of (*E*)-2HBAMBA.

4.3.1. O–H vibrations

The O–H stretching vibrations are sensitive to hydrogen bonding. The non-hydrogen bonded (or) free hydroxyl group absorb strongly in 3550–3700 cm^{-1} region [36]. The vibrational band found at 3803, 3690 cm^{-1} in FT-IR (3655, 3594 cm^{-1}: B3LYP mode nos.: ν_1, ν_2), can be assigned as O–H stretching. Infrared observed band at 3699 and 3662 cm^{-1} for 2,3-dihydroxy pyridine [37] which agrees well with the observed band in the present study. These assignments are supported by TED (100%) and also within the expected range [36]. In (*E*)-2HBAMBA, the observed FT-IR bands 1173 and 1085 cm^{-1} are assigned to O–H in-plane bending. Krishnakumar and Muthunatesan [37] identified the β O–H vibrations at 1188, 1123, 1047 cm^{-1} in the case of 2,3-dihydroxy pyridine. These assignments are agreeable with harmonic values: 1153, 1089 cm^{-1} (B3LYP/mode nos.: ν_{39}, ν_{43}). It is evident from TED column in Table 3, the β O–H vibrations are mixed with C–C vibrations. A pure mode cannot be expected for Γ O–H vibration as it falls in a mixed vibration of vibrational spectrum. The theoretical wave numbers of this band 726, 611, 440, 401 and 389 cm^{-1} (B3LYP/mode nos.: ν_{59}, ν_{63}, ν_{69-71}) coincides well with experimental (FT-IR: 716, 611, 440 and Raman: 396 cm^{-1}) as well as characteristic value (625 cm^{-1}) reported by Akkaya and Akyüz [38] for 4-amino-salicylic acid.

4.3.2. C–H vibrations

The heteroaromatic structure shows the presence of C–H stretching vibrations in the range 3000–3100 cm^{-1} range which is the characteristic region for the ready identification of C–H stretching vibrations [39]. If the C–H bond is adjacent to an aromatic ring, the C–H stretching frequency and absorption between 3100 cm^{-1} and 3000 cm^{-1} can be expected [40]. The phenyl ring C–H vibrations is observed at 3095 cm^{-1} as broad and low intense band in FT-IR spectra. The scaled vibrational mode nos.: ν_{3-6} corresponds to stretching mode (3087–3039 cm^{-1}/B3LYP) of C–H units for (*E*)-2HBAMBA. These assignments are further supported by TED (100%). These experimental and theoretical wavenumbers of C–H stretching vibration is well coincided with literature [34,41,42]. In aromatic compounds, the C–H in-plane bending wavenumbers appear in the range 1000–1300 cm^{-1} and the C–H out-of-plane bending vibration in the range 750–1000 cm^{-1} [39,43,44]. The C–H in-plane and C–H out-of-plane 4-amino-salicylic acid are assigned to 1369, 1228, 1108 cm^{-1} and 819–970 cm^{-1}, respectively, by Akkaya and Akyüz [38]. The bands are observed at 1229, 1150, 1068 cm^{-1} and 962, 781 cm^{-1} belong to C–H in-plane and out-of-plane bending, respectively, for 3-amino-salicylic acid [45]. The C–H in-plane bands are sharp but weak to medium intensity. The weak bands at 1295, 1236, 1181, 1140 in FT-IR spectrum are due to in-plane C–H bending. The same vibration appears in the FT-Raman spectrum at 1295, 1236, 1181 with weak intensity. The theoretically computed values for β C–H also falls in the region 1289–1072 cm^{-1} (mode nos.: ν_{32}, ν_{36-38}, ν_{40}, ν_{44}) by B3LYP/6-31G(d,p) method. The out-of-plane bending vibration of C–H assigned at 942, 833, 746 cm^{-1} and at 964, 946 in FT-Raman spectrum. These assignments are satisfactorily coinciding with the

computed values of the mode nos.: ν_{47}, ν_{48}, ν_{55}, ν_{58} (B3LYP). The above assignments are also supported by the literature [44] in addition to TED output. The calculated bands in the range 2908–2845 cm^{-1} (B3LYP/mode nos.: ν_{13-15}) and observed bands 2896, 2868 cm^{-1} (both: FT-IR/FT-Raman) are attributed to C–H stretching in the present molecule other than phenyl ring.

4.3.3. Methyl group vibrations

Methyl groups are generally referred to as electron donating substituents in the aromatic ring system [46]. The title compound (*E*)-2HBAMBA, posses two CH_3 groups attached to the C_{14} atom. For the assignments of CH_3 group frequencies one can expect nine fundamentals which can be associated to each CH_3 group, namely the symmetrical stretching in CH_3 (CH_3 symmetric stretching) and a symmetrical stretching (CH_3 asymmetric stretching), in-plane stretching modes (i.e. in-plane hydrogen stretching mode), the symmetrical (CH_3 symmetric deformation) and asymmetrical (CH_3 asymmetric deformation) deformation modes, the in-plane rocking (CH_3 ipr), out-of-plane rocking (CH_3 opr) and twisting (t CH_3) bending modes. The C–H stretching appeared at lower frequencies than those of the aromatic ring (3000 cm^{-1}). For the CH_3 compounds, the mode ν_{sym} appears in the range 2860–2935 cm^{-1}, where as the ν_{asy} modes appear in the region 2925–2985 cm^{-1} [47]. In the present study, the methyl group symmetric stretching vibrations are established at 2932 cm^{-1} in both FT-IR and FT-Raman spectra, while the calculated wave numbers are 2931, 2923 cm^{-1} (B3LYP mode nos.: ν_{11}, ν_{12}). Similarly the observed bands: 2994, 2954 cm^{-1} (FT-IR) and computed wave numbers: 2992, 2991 cm^{-1} (B3LYP/mode nos.: ν_9, ν_{10}) are attributed to CH_3 asymmetric stretching mode. These assignments are in the expected range and also supported by Abraham et al. [48] for p-amino acetanilide and Koleva et al. [49]. The asymmetric and symmetric bending vibrations of methyl groups normally appear in the region 1465–1440 cm^{-1} and 1390–1370 cm^{-1}, respectively [50,51]. The calculated wavenumbers in the range 1467–1444 cm^{-1} (B3LYP/mode nos.: ν_{21-24}) and 1383, 1367 (B3LYP/mode nos.: ν_{27}, ν_{28}) are attributed to CH_3 asymmetric and CH_3 symmetric bending modes, respectively. These assignments are supported by TED and also in line with observed FT-IR: 1470, 1455 and 1370, and FT-Raman: 1470, 1453 cm^{-1} bands. The scissoring mode of CH_3 (δ), lies in the range of 1467–1444 cm^{-1} (B3LYP) is well reproduced by FT-IR (1470, 1455 cm^{-1}) and FT-Raman (1470, 1453 cm^{-1}). The wagging and rocking deformation of methyl groups have observed at 1181 cm^{-1} (FT-IR, FT-Raman) and 1131 (FT-IR), 925 cm^{-1} (FT-Raman), respectively. Similarly, the theoretical investigation lies about 1161 and 1126, 924 cm^{-1} for wagging (ω) and rocking (ρ), respectively, these modes are in good agreement with experimental values. The intensity enhancement and blue shifting of the methyl stretching wavenumbers are due to the inference of electronic effect resulting from the hyperconjugation and induction of methyl group in-the aromatic ring [52].

4.3.4. C=O, C–O vibrations

Vibrational analysis of carboxylic acid is made on the basis of carbonyl and hydroxyl group. The carbonyl stretching frequency has been most extensively studied by infrared spectroscopy [52]. This multiply bonded group is highly polar and therefore gives rise to an intense infrared absorption band. The carbon–oxygen double bond is formed by Pπ–Pπ bonding between carbon and oxygen. Because of the different electro negativities of carbon and oxygen atoms, the bonding electrons are not equally distributed between the two atoms. The following two resonance forms contribute to the bonding of the carbonyl group $>C{=}O \leftrightarrow C^{+}{-}O^{-}$. The lone pair of electrons on oxygen also determines the nature of the carbonyl group. The C=O stretch of carboxylic acids is identical to the C=O stretch of ketones, which is expected in the region 1740–1660 cm^{-1} [53]. In this work, C=O stretching vibration has a main contribution in the mode no. 16, with B3LYP/6-31G(d,p) predicted frequency of 1776 cm^{-1} and the values are observed at 1616 cm^{-1} (strong), the shifting of keto (C=O) group frequency is due to intra-molecular interaction between hydrogen of hydroxyl and nitrogen atom. This is in agreement with James et al. [53] in the case of (2-methyphenoxy) acetic acid dimer and further it is supported by TED (86%). The νC–O and $\nu_{aromatic}$ C–O (C–O group attached with phenyl ring) are assigned at 1275/1257 and 1242/1257 cm^{-1} (IR/Raman), respectively, by James et al. [53]. The harmonic bands 1126, 1106 and 1273, 1263 cm^{-1} (B3LYP/6-31G(d,p)): mode nos.: ν_{41}, ν_{42}, ν_{34}, ν_{35}) are attributed to νC–O and $\nu_{aromatic}$ C–O mode, respectively. The corresponding νC–O mode is observed at 1131 cm^{-1} with strong intensity in FT-IR while the FT-Raman: 1130 cm^{-1} is weak. Significant intensity enhancement in FT-IR is due to the conjugation with ring π system. This FT-IR band show an agreement with literature [33,41].

The βC=O vibrational mode with the theoretical frequency of 671 cm^{-1} (B3LYP) mode no.: 61) agrees well with experimental (FT-IR/FT-Raman) values at 684/684 cm^{-1} values. The above conclusion is in agreement with literature value [53]. The theoretically calculated value by B3LYP/6-31G(d,p) method at 440 cm^{-1} (mode no.: ν_{69}) shows an excellent agreement with experimental FT-IR data 440 cm^{-1} and is designated as γC=O bending. The FT-IR bands identified at 833 and 746 cm^{-1} are assigned to ωC–O mode, these are in line with harmonic values 818, 735 cm^{-1} (B3LYP/mode nos.: ν_{55}, ν_{58}) and are further supported by earlier study [54]. Literature survey reveals that the βO–C–O assigned at 649 cm^{-1} in the case of p-bromoacetic acid [55]. The δO–C–O and γO–C–O modes contribute (respectively in 13% and 10%) to the bands observed, respectively, at 641 (B3LYP/mode no.: 62) and 440 cm^{-1} (B3LPY/ mode no.: 69). This is in reasonable agreement with the observed FT-IR (670 and 440 cm^{-1}) bands. According to the work by Sundaraganesan [55] on p-bromoacetic acid the harmonic wavenumbers at 1280, 1122 and 505 cm^{-1} are assigned to the δC–O–H and ΓC–O–H, respectively. In this study, these vibrations are observed in the range 1106–1289 cm^{-1} and 389–726 cm^{-1}, respectively. These assignments are in line with the experimental values.

4.3.5. C=N and C–N vibrations

The identification of C=N and C–N vibrations are the very difficult task, since the mixing of several bands are possible in the region [39]. The C=N stretching appears in the region 1600–1670 cm^{-1}[56]. Khalaji et al. [34] recorded the C=N (aromatic) stretching band at 1490–1570 cm^{-1}. The observed intense band at 1586 cm^{-1} (strong) in FT-IR is assigned to the C=N stretching mode. For the same mode the calculated frequency 1662 cm^{-1} (B3LYP/mode no.: 17) is positively deviated ($\sim$76 cm^{-1}) from the observed value. This is supported by TED (78%) value. According to the literature [33–35] the C=N stretching mode is also shifted to lower region (1586 cm^{-1}). Shifting of C=N frequency is due to π electron transfer from N to O atom through intra-molecular interaction. Silverstein et al. [39] assigned C–N stretching absorption in the region 1266–1382 cm^{-1} for aromatic amines. In (*E*)-2HBAMBA the band observed at 1036 cm^{-1} (FT-IR) is attributed to C–N stretching. The bands at 1039 (mode no.: ν_{45}) and 320, 276 cm^{-1} (B3LYP/mode nos.: ν_{74}, ν_{75}) are due to βC–N and ΓC–N bending modes, respectively.

4.4. Thermodynamic properties

Several calculated thermodynamic parameters are presented in Table 4. Scale factors have been recommended [57] for an accurate prediction in determining the zero-point vibrational energies

Table 4
Theoretically computed energies, zero-point vibrational energies (kcal/mol), rotational constants (GHz), entropy (cal/mol K^{-1}) and dipole moment (D) for (E)-2HBAMBA.

Parameters	B3LYP/6-31G(d,p)
Total energies	−746.78
Zero point energy	160.27
Rotational constants	1.1172
	0.2534
	0.2488
Entropy	
Total	127.00
Translational	42.08
Rotational	32.79
Vibrational	52.13

Table 5
The electric dipole moment (μDebye), polarizability (α in $\times 10^{-30}$ esu), hyper polarizability (β_0 in $\times 10^{-30}$ esu) values of (E)-2HBAMBA.

Parameters	B3LYP/6-31G(d,p)
Dipole moment	
μ_x	0.398
μ_y	−1.288
μ_z	−0.187
μ	1.361
Polarizability	
α_{xx}	220.2
α_{xy}	−0.20
α_{yy}	135.7
α_{xz}	−2.36
α_{yz}	13.40
α_{zz}	90.77
α	0.386
Hyperpolarizability	
β_{xxx}	306.4
β_{xxy}	−159.4
β_{xyy}	−31.90
β_{yyy}	−109.7
β_{xxz}	−107.8
β_{xyz}	−33.70
β_{yyz}	39.64
β_{xzz}	62.85
β_{yzz}	−0.45
β_{zzz}	14.77
β_0	0.376

(ZPVE), and the entropy, S_{vib} (T). The variations in the ZPVEs seem to be insignificant.

5. Hyperpolarizability calculations

The first hyperpolarizabilities (β, α_0 and $\Delta\alpha$) of (E)-2HBAMBA is calculated using B3LYP/6-31G(d,p) basis set, based on the finite-field approach. In the presence of an applied electric field, the energy of a system is a function of the electric field. First hyperpolarizability is a third rank tensor that can be described by a $3 \times 3 \times 3$ matrix. The 27 components of the 3D matrix can be reduced to 10 components due to Kleinman symmetry [58]. It can be given in the lower tetrahedral format. It is obvious that the lower part of the $3 \times 3 \times 3$ matrixes is a tetrahedral. The components of β are defined as the coefficients in the Taylor series expansion of the energy in the external electric field. When the external electric field is weak and homogeneous, this expansion becomes:

$$E = E^0 - \mu_\alpha F_\alpha - \frac{1}{2\alpha_{\alpha\beta}F_\alpha F_\beta} - \frac{1}{6\beta_{\alpha\beta\gamma}F_\alpha F_\beta F_\gamma} \quad (2)$$

where E^0 is the energy of the unperturbed molecules, F_α the field at the origin, and μ_α, $\alpha_{\alpha\beta}$, $\beta_{\alpha\beta\gamma}$ are the components of the dipole moment, polarizability and the first hyperpolarizabilities, respectively. The total static dipole moment μ, the mean polarizability α_0, the anisotropy of polarizability $\Delta\alpha$ and the mean first hyperpolarizability β_0, using the x, y, z components are defined as

$$\mu = (\mu_x^2 + \mu_y^2 + \mu_z^2)^{1/2} \quad (3)$$

$$\alpha_0 = \frac{\alpha_{xx} + \alpha_{yy} + \alpha_{zz}}{3} \quad (4)$$

$$\Delta\alpha = 2^{-1/2}[(\alpha_{xx} - \alpha_{yy})^2 + (\alpha_{yy} - \alpha_{zz})^2 + (\alpha_{zz} - \alpha_{xx})^2 + 6(\alpha_{xy}^2 + \alpha_{yz}^2 + \alpha_{xz}^2)]^{1/2} \quad (5)$$

$$\beta_0 = (\beta_x^2 + \beta_y^2 + \beta_z^2)^{1/2} \quad (6)$$

The total molecular dipole moment (μ) and mean first hyperpolarizability (β_0) are of (E)-2HBAMBA is about 1.3619 Debye and 0.3760×10^{-30} esu, respectively. The total dipole moment and the first hyperpolarizability (β_0) of the title molecule is nearly same as

Table 6
The NBO analysis of (E)-2HBAMBA.

Type	Donor (i)	ED/e	Acceptor (j)	ED/e	$E^{(2)}$ (kJ/mol)
σ–σ*	C_1–C_6	1.979	C_1–C_2	0.024	9.54
			C_1–H_7	0.012	5.98
			C_2–O_{29}	0.018	14.39
			C_5–C_6	0.016	10.38
			C_5–H_9	0.012	9.25
			C_6–H_{10}	0.012	4.60
π–π*	C_1–C_6	1.702	C_4–C_5	0.316	67.40
σ–σ*	C_4–C_5	1.980	C_3–C_4	0.020	12.43
π–π*	C_4–C_5	1.709	C_1–C_6	0.310	91.21
π–π*	C_{11}=N_{31}	1.945	C_{13}–C_{14}	0.037	16.57
			C_{13}–C_{21}	0.079	11.59
n–π*	LPC2	1.999	C_1–C_6	0.310	220.71
			C_4–C_5	0.014	2.89
n–π	LPC3	1.999	C_4–C_5	0.316	285.52
			C_{11}–N_{31}	0.175	284.26
n–π	LPO22	1.999	C_{13}–C_{21}	0.079	10.54
n–π*	LPO22	1.839	C_{13}–C_{21}	0.079	85.52
			C_{21}–O_{23}	0.104	144.10
n–π	LPO23	1.976	C_{21}–O_{22}	0.022	30.38
n–π*	LPO23	1.815	C_{21}–O_{22}	0.207	197.61
n–π	LPN31	1.860	C_3–C_{11}	0.026	10.50
			O_{29}–H_{30}	0.074	123.47

$E^{(2)}$ means energy of hyperconjugative interactions (stabilization energy).

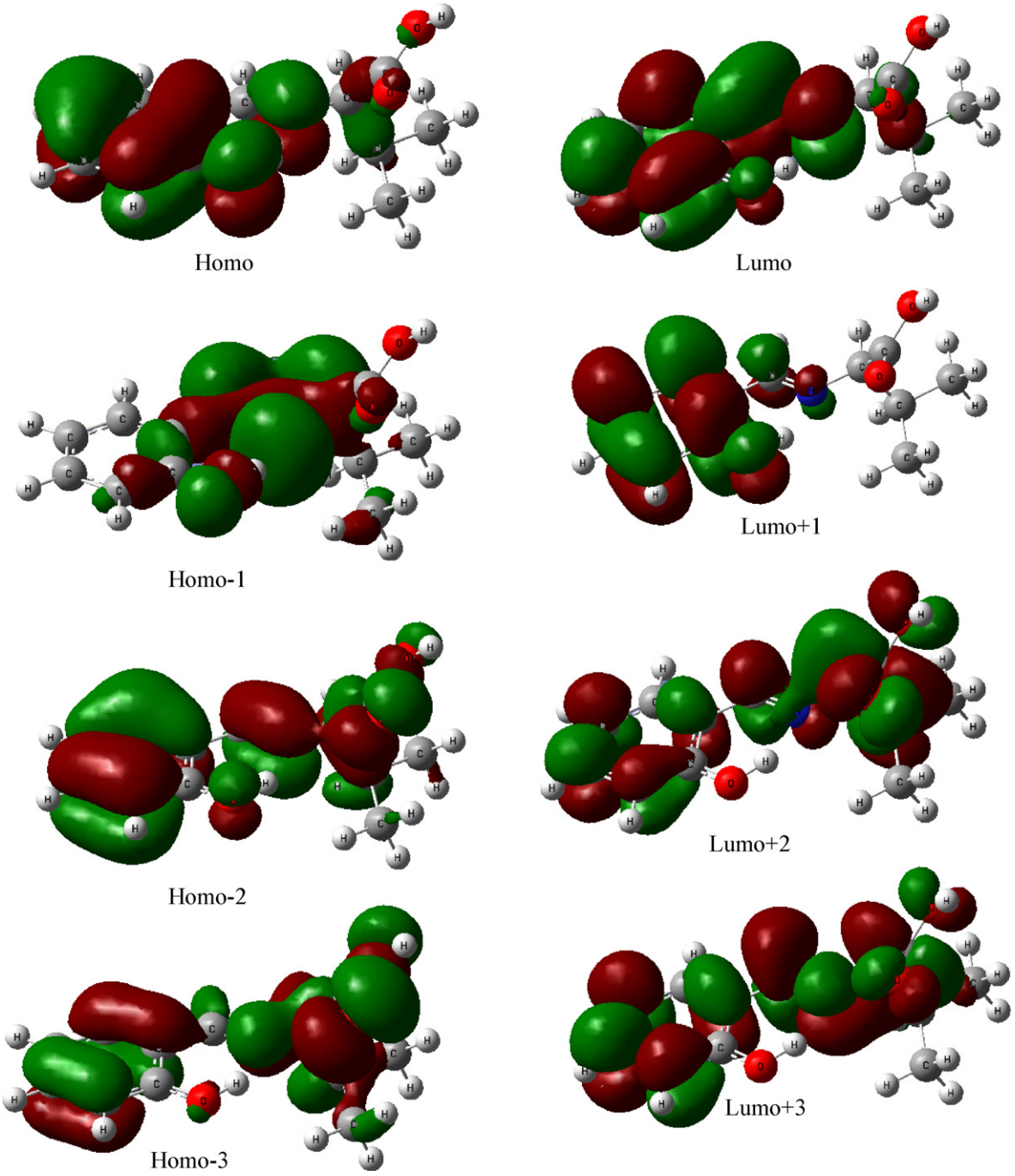

Fig. 5. The frontier molecular orbital of (*E*)-2HBAMBA.

of urea, hence this molecule has considerable NLO activity (μ and β of urea are 1.3732 Debye and 0.3728×10^{-30}). The computation of the molecular polarizability of (*E*)-2HBAMBA is shown in Table 5.

6. NBO analysis

The hyperconjugation may be given as stabilizing effect that arises from an overlap between an occupied orbital with another neighboring electron deficient orbital, when these orbitals are properly orientated. This non-covalent bonding–antibonding interaction can be quantitatively described in terms of the NBO analysis, which is expressed by means of the second-order perturbation interaction energy ($E^{(2)}$) [59–62]. This energy represents the estimate of the off-diagonal NBO Fock matrix elements. It can be deduced from the second-order perturbation approach [63]:

$$E^{(2)} = \Delta E_{ij} = q_i \frac{F(i,j)^2}{\varepsilon_j - \varepsilon_i} \quad (7)$$

where q_i is the donor orbital occupancy, ε_i and ε_j are diagonal elements (orbital energies) and $F(i, j)$ is the off diagonal NBO Fock matrix elements. In this present investigation studied the charge transfers from one bond to another bond. The bonds σC1–C6 and πC1–C6 have the electron density about 1.979 and 1.702e, respectively, which stabilizes 9.54 and 67.40 kJ/mol to its antibonding orbitals of σ*C1–C2 and π*C4–C5, respectively. Investigating the π bond over the molecule, more energy transfer

Table 7
The electronic transition of (*E*)-2HBAMBA.

Calculated at B3LYP/6-311++G(d,p)	Oscillator strength	Calculated band gap (eV/nm)
Excited state 1	Singlet A (f = 0.1068)	3.9267 eV, 315.75 nm
58 -> 60 (Homo$_{-1}$–Lumo)		5.356
58 -> 63 (Homo$_{-1}$–Lumo$_{+3}$)		5.567
59 -> 60 (Homo–Lumo)		4.498
Excited state 2	Singlet A (f = 0.0032)	4.6415 eV, 267.12 nm
57 -> 60 (Homo$_{-2}$–Lumo)		5.957
Excited state 3	Singlet A (f = 0.3124)	4.8600 eV, 255.11 nm
58 -> 60 (Homo$_{-1}$–Lumo)		5.3563
59 -> 62 (Homo–Lumo$_{+2}$)		5.6445
59 -> 63 (Homo–Lumo$_{+3}$)		4.7092

takes place during π to π* transition. In this molecule the π bonds of C4–C5 and C11–N31 transfers 91.21 and 16.57 kJ/mol to the antibonding acceptor orbitals. The C=N group energy transfer differs when there is change in the position of hydrogen. It is evident from Table 6, the hydroxyl group hydrogen is outwards from nitrogen, the C=N bond transfers 32.55 kJ/mol to acceptor of C2–C3 orbital, when hydrogen is towards the nitrogen, the intramolecular interaction takes place between the C=N and O–H group (O–H···N = C), hence the LPN31–π transfer has more energy to acceptor of π*–O29–H30 (123.47 kJ/mol). There is also calculated a lesser energy transfer from LPN31 to C3–C11 (10.50 kJ/mol). The intra-molecular interaction is found between two electronegative atoms (O29–H30···N31), the interaction distance about 1.722 Å (B3LYP). The lone pair of atoms have more energy stabilization about 220.71 (LPC2 → π*C1–C6), 285.52 (C3 → C4–C5), 197.61 (O23 → C21–C22) and 123.47 kJ/mol (N31 → O29–H30).

7. Homo–Lumo band gap

Table 7 shows the electronic transition of (*E*)-2HBAMBA, calculated by TD-B3LYP/6-311++G(d,p) method. In which computed electronic transition energies and their oscillator strength were listed. Among and calculated electronic transition, the first excited state consist three singlet states in 315.75 nm range, with a 0.1068 oscillator strength. Calculated band gap of this state is about 3.9267 eV. In singlet-A (excited state1), 58 → 60 (Homo$_{-1}$–Lumo), 58 → 63 (Homo$_{-1}$–Lumo$_{+3}$) and 59 → 60 (Homo–Lumo) are involved. The second excited state lies in the range of 267.12 nm, with a 0.0032 oscillator strength, involved orbital is 57 → 60 (Homo$_{-2}$–Lumo) and its band gap is about 4.6415 eV. There were three energy levels appeared at 3rd excited state in 255.11 nm range, with a oscillator strength of 0.3124, this includes 58 → 60 (Homo$_{-1}$–Lumo), 59 → 62 (Homo–Lumo$_{+2}$) and 59 → 63 (Homo–Lumo$_{+3}$) as a excited states. Band gap energy of 3rd excited state is about 4.8600 eV. In above discussion, the homo is mainly locates over the phenol ring and C=N group, homo$_{-1}$ located around C–N=C, and Homo$_{-2}$ appears at C–C–C, C=N and C=O group. Orbital 60, 61 have localized its electron density around each atom of phenol ring and orbital 62, 63 localized its electron density over each atom of molecule with some exception of hydroxyl and methyl groups. The Homo and Lumo plots are shown in Fig. 5.

8. Conclusion

The studied molecule (schiff base) was newly synthesized and it was optimized by B3LYP with 6-31G(d,p) method. Optimized bond parameters were compared with available literatures and it shows a good agreement. Theoretical investigation had shown that the intra-molecular interaction was formed between (O29–H30···N31) O29 and N31 atoms. Their calculated interaction bond distance was about 1.722 Å (B3LYP) method. The FT-IR, FT-Raman and UV–vis spectrum was recorded; the recorded spectral results were compared with computed values. Using the total energy distribution (TED), the complete vibrational analysis was carried out. During the intramolecular hydrogen bonding interaction the hyperconjugative interaction (LPN31 → O29–H30) energy ($E^{(2)}$) was calculated about 123.47 kJ/mol using NBO (B3LYP/6-31G(d,p)) analysis. The excited states one, two and three were calculated by TD-DFT/6-311++G(d,p) method. The first, second and third excited states are lies about 315.75, 267.12 and 255.11 nm range and their corresponding band gap energy was about 3.9267, 4.6415 and 4.8600 eV, respectively.

References

[1] M.S. Karthikeyan, D.J. Prasad, B. Poojary, K.S. Bhat, B.S. Holla, N.S. Kumari, Bioorg. Med. Chem. 14 (2006) 7482–7489.
[2] R. Lozier, R.A. Bogomolni, W. Stoekenius, J. Biophys. 15 (1975) 955–962.
[3] A.D. Garnovski, A.L. Nivorozhkin, V.I. Minkin, Coord. Chem. Rev. 126 (1993) 1.
[4] Y.Z. Xiong, F.E. Chen, J. Balzarini, E.D. Clercq, C. Pannecouque, Eur. J. Med. Chem. 43 (2008) 1230–1236.
[5] D. Sriram, P. Yogeeswari, N. Sirisha, V. Saraswat, Bioorg. Med. Chem. Lett. 16 (2006) 2127–2129.
[6] H. Zhao, N. Neamati, S. Sunder, H. Hong, S. Wang, G.W.A. Milne, Y. Pommier, T.R. Burke, J. Med. Chem. 40 (1997) 937–941.
[7] G. Liu, J. Peiliao, S. Huang, G. Lishen, R. Qinyu, Anal. Sci. 17 (2001) 1031–1035.
[8] A.D. Khalaji, M. Amirnasr, S. Triki, Inorg. Chim. Acta 362 (2009) 587–590.
[9] M. Morshedi, M. Amirnasr, A.M.Z. Slawin, D.J. Woollins, A.D. Khalaji, Polyhedron 28 (2009) 167–171.
[10] M. Morshedi, M. Amirnasr, S. Triki, A.D. Khalaji, Inorg. Chim. Acta 362 (2009) 1637–1640.
[11] A.D. Khalaji, H. Hadadzadeh, K. Gotoh, H. Ishida, Acta Cryst. E65 (2009) m70.
[12] J.W. Williams, A. Sadle, J. Am. Chem. Soc. 62 (1940) 2801–2803.
[13] L. Sacconi, I. Bertini, Inorg. Chem. 5 (1966) 1520–1522.
[14] Z.S. Sales, N.S. Mani, J. Org. Chem. 74 (2009) 891–894.
[15] P.H. Wang, J.G. Keck, E.J. Lien, M.M.C. Lai, J. Med. Chem. 33 (1990) 608–614.
[16] G.M. Chinigo, M. Paige, S. Grindrod, E. Hamel, S. Dakshanamurthy, M. Chruszcz, W. Minor, M.L. Brown, J. Med. Chem. 51 (2008) 4620–4631.
[17] M.M. Abd-Elzaher, S.A. Moustafa, A.A. Labib, M.M. Ali, Monatsh. Chem. Chem. Mon. 141 (2010) 387–393.
[18] V.I. Prisakar, V.I. Tsapkov, S.A. Buracheéva, M.S. Byrké, A.P. Gulya, J. Pharm. Chem. 39 (2005) 313–315.
[19] L. Lazzarato, M. Donnola, B. Rolando, E. Marini, C. Cena, G. Coruzzi, E. Guaita, G. Morini, R. Fruttero, A. Gasco, S. Biondi, E. Ongini, J. Med. Chem. 51 (2008) 1894–1903.
[20] E. Hadjoudis, M. Vitterakis, I.M. Mavridis, Tetrahedron 43 (1987) 1345–1360.
[21] I.M. Mavridis, E. Hadjoudis, A. Mavridis, Acta Crystallogr. B 36 (1980) 1126–1130.
[22] K.V. Gothelf, A. Thomsen, M. Nielsen, E. Clo, R.S. Brown, J. Am. Chem. Soc. 126 (2004) 1044–1046.
[23] G. Chung, O. Kwon, Y. Kwon, J. Phys. Chem. A 102 (1998) 2381–2387.
[24] A. Chandran, Y.S. Mary, H.T. Varghese, C.Y. Panicker, P. Pazdera, G. Rajendran, N. Babu, J. Mol. Struct. 992 (2011) 77–83.
[25] E.S. Howard, E.P. Burrows, M.J. Marks, R.D. Lynch, F.-M. Chen, J. Am. Chem. Soc. 99 (1977) 707–713.
[26] Spartan 08, Wavefunction Inc., Irvine, CA 92612, USA, 2008.
[27] M.J. Frisch, G.W. Trucks, H.B. Schlegel, G.E. Scuseria, M.A. Robb, J.R. Cheeseman, J.A. Montgomery Jr., T. Vreven, K.N. Kudin, J.C. Burant, J.M. Millam, S.S. Iyengar, J. Tomasi, V. Barone, B. Mennucci, M. Cossi, G. Scalmani, N. Rega, G.A. Petersson, H. Nakatsuji, M. Hada, M. Ehara, K. Toyota, R. Fukuda, J. asegawa, M. Ishida, T. Nakajima, Y. Honda, O. Kitao, H. Nakai, M. Klene, X. Li, J.E. Knox, H.P. Hratchian, J.B. Cross, C. Adamo, J. Jaramillo, R. Gomperts, R.E. Stratmann, O. Yazyev, A.J. Austin, R. Cammi, C. Pomelli, J.W. Ochterski, P.Y. Ayala, K. Morokuma, G.A. Voth, P. Salvador, J.J. Dannenberg, V.G. Zakrzewski, S. Dapprich, A.D. Daniels, M.C. Strain, O. Farkas, D.K. Malick, A.D. Rabuck, K. Raghavachari, J.B. Foresman, J.V. Ortiz, Q. Cui, A.G. Baboul, S. Clifford, J. Cioslowski, B.B. Stefanov, G. Liu, A. Liashenko, P. Piskorz, I. Komaromi, R.L. Martin, D.J. Fox, T. Keith, M.A. Al-Laham, C.Y. Peng, A. Nanayakkara, M. Challacombe, P.M.W. Gill, B. Johnson, W. Chen, M.W. Wong, C. Gonzalez, J.A. Pople, Gaussian 03, Revision E.01, Gaussian Inc., Pittsburgh, PA, 2003.
[28] H.B. Schlegel, J. Comput. Chem. 3 (1982) 214–218.
[29] G. Rauhut, P. Pulay, J. Phys. Chem. 99 (1995) 3093–3100.
[30] A. Frisch, A.B. Nielson, A.J. Holder, GAUSSVIEW User Manual, Gaussian Inc., Pittsburgh, PA, 2000.
[31] D. Michalska, Raint Program, Wroclaw University of Technology, 2003.
[32] D. Michalska, R. Wysokinski, Chem. Phys. Lett. 403 (2005) 211–217.
[33] B. Koar, C. Albayraka, M.O. Daba oglub, O. Büyükgüngör, Crystallogr. Rep. 55 (2010) 1207–1210.
[34] A.D. Khalaji, A.N. Chermahini, K. Fejfarova, M. Dusek, Struct. Chem. 21 (2010) 153–157.
[35] N. Tezer, N. Karakus, J. Mol. Model. 15 (2009) 223–232.

[36] K. Bahgat, A.G. Ragheb, Cent. Eur. J. Chem. 5 (2007) 201–220.
[37] V. Krishnakumar, S. Muthunatesan, Spectrochim. Acta A 65 (2006) 818–825.
[38] Y. Akkaya, S. Akyüz, Vib. Spectrosc. 42 (2006) 292–301.
[39] M. Silverstein, G. Clayton Basseler, C. Morill, Spectrometric Identification of Organic Compounds, Wiley, New York, 1981.
[40] J.P. Abraham, Spectrochim. Acta A 71 (2008) 355–367.
[41] O.V. Kotova, S.V. Eliseeva, A.S. Averjushkin, L.S. Lepnev, A.A. Vaschenko, A.Yu. Rogachev, A.G. Vitukhnovskii, N.P. Kuzmina, Russ. Chem. Bull. Int. Ed. 57 (2008) 1880–1889.
[42] M. Boczar, M.J. Wójcik, Krzysztof szczeponek, Dorota jamróz, Susumu ikeda, Int. J. Quant. Chem. 90 (2002) 689–698.
[43] G. Socrates, Infrared and Raman Characteristic Group Frequencies. Tables and Charts, third ed., Wiley, Chichester, 2001.
[44] G. Varsanyi, Assignments of Vibrational Spectra of 700 Benzene Derivatives, Wiley, New York, 1974.
[45] H.I.S. Nogueira, Spectrochim. Acta A 54 (1998) 1461–1470.
[46] W.B. Tzeng, K. Narayanan, J.L. Lin, C.C. Tung, Spectrochim. Acta 55A (1999) 153.
[47] N. Sundaraganesan, C. Meganathan, H. Saleem, B. Dominic Joshua, Spectrochim. Acta A 68 (2007) 619–625.
[48] J. Abraham, D. Sajan, I. Hubert Joe, V.S. Jayakumar, Spectrochim. Acta 71A (2008) 355–367.
[49] B.B. Koleva, R.D. Nikolova, S. Zareva, T. Kolev, A.G. Bojilova, H. Mayer-Figge, W.S. Sheldrick, Struct. Chem. 19 (2008) 975–982.
[50] N.B. Coithup, L.H. Daly, S.E. Wiberley, Introduction to Infrared and Raman Spectroscopy, Academic Press, New York, 1990.
[51] G. Socrates, Infrared Characteristic Group Frequencies, Wiley-Interscience Publication, New York, 1980.
[52] Y. Hung, D.F.R. Gilson, I.S. Butlei, J. Chem. Phys. 97 (1993) 1998.
[53] C. James, C. Ravikumar, T. Sundis, V. Krishnakumar, R. Kesavamoorthy, V.S. Jayakumar, I. Hubert Joe, Vib. Spectrosc. 47 (2008) 10–20.
[54] V. Krishnakumar, N. Surumbarkuzhali, J. Raman Spectrosc. 41 (2010) 473–478.
[55] N. Sundaraganesan, C. Meganathan, B. Anand, Christine Lapouge, Spectrochim, Acta. 66 (2007) 773–780.
[56] G. Socrates, Infrared Characteristic Group Frequencies, John Wiley and Sons Ltd., New York, 1980.
[57] M.A. Palafox, Int. Quant. J. Chem. 77 (2000) 661.
[58] N.B. Colthup, L.H. Daly, S.E. Wiberly, Introduction to Infrared and Raman Spectroscopy, Academic Press, New York, 1990.
[59] A.E. Reed, F. Weinhold, J. Chem. Phys. 83 (1985) 1736–1740.
[60] A.E. Reed, R.B. Weinstock, F. Weinhold, J. Chem. Phys. 83 (1985) 735–746.
[61] A.E. Reed, F. Weinhold, J. Chem. Phys. 78 (1983) 4066–4073.
[62] J.P. Foster, F. Wienhold, J. Am. Chem. Soc. 102 (1980) 7211–7218.
[63] J. Chocholousova, V. Vladimir Spirko, P. Hobza, Phys. Chem. Chem. Phys. 6 (2004) 37–41.